as follows. Multiplication by K' and simplification of the right-hand side yield eq A-6. Although the quantity K' is not

$$K' \ln [i/(i_{eq} - i)] = k_f' t \qquad \text{(A-6)}$$

directly measurable because it equals (P_{eq}), it is directly proportional to i_{eq}, the limiting current at equilibrium, and thus can be replaced by Ai_{eq} where A is an (unknown) proportionality constant. Making this substitution in eq A-6 and rearranging yield eq A-7, which, by permitting determination

$$i_{eq} \ln [i/(i_{eq} - i)] = k_f' t/A \qquad \text{(A-7)}$$

of the quantity k_f'/A for different reactant concentrations, allows establishment of the order of the forward reaction with respect to each reactant.

Registry No. ReO_4^-, 14333-24-5; citric acid, 77-92-9; oxalic acid, 144-62-7.

Contribution from the Department of Chemistry, University of Maryland, College Park, Maryland 20742, and the Department of Geological Sciences, University of Aston in Birmingham, Birmingham, England B4 7ET

Relationships between Valence Orbital Binding Energies and Crystal Structures in Compounds of Copper, Silver, Gold, Zinc, Cadmium, and Mercury

J. A. TOSSELL* and D. J. VAUGHAN

Received January 10, 1981

Theoretical calculations and X-ray spectral data are used to determine the relative binding energies of the Cu, Ag, Au, Zn, Cd, and Hg d orbitals and the ligand p orbitals in the metal chlorides and sulfides. Compared to the S 3p nonbonding orbitals, the metal d orbitals are of lower binding energy for Cu, of slightly higher binding energy for Au, Ag, and Hg, and of considerably higher binding energy for Zn and Cd. Transformation from gaseous monomer to gaseous polymer to condensed phase is shown to raise the metal (M) d orbital energy with respect to the ligand (L) p, resulting in a larger L p–M d energy separation and smaller L p–M d covalent mixing for Cu compounds and a smaller separation and greater covalent mixing for compounds of the other metals. The existence or nonexistence of different oxidation states of these metals in combination with various ligands can be qualitatively understood on the basis of the energies of predominantly M d and L p orbitals obtained from spectra or molecular cluster calculations (and to some extent from the M d and L p atomic orbital energies). Similarly, the coordination numbers and polyhedral distortions in the most stable polymorphs of these compounds are determined by the numbers of M d electrons and the extent of M d–L p covalent mixing. The adoption of structures with low M coordination numbers by compounds with filled M d shells and small M d–L p energy differences serves to lower the M d energy and reduce the destabilization due to M d–L p covalent mixing.

Introduction

Compounds of metals near the ends of the transition series often exhibit unusual structures even for binary phases.[1] For example, Cu_2O adopts the cuprite structure in which Cu^I is two-coordinate, CuO adopts the tenorite structure in which Cu^{II} is four-coordinate square planar, Cu_2S adopts the complex chalcocite structure in which the Cu exists in (distorted) three-coordination, and CuS adopts the very unusual covellite structure, in which the Cu is partly three-coordinate and partly four-coordinate and in which disulfide anions, S_2^{2-}, occur. Even the copper fluorides are not simple—solid CuF has apparently never been prepared and CuF_2, although it has the common rutile structure, has Cu in a highly distorted six-coordinate (or 4 + 2) site. Compounds of heavier elements in the Cu group also have unusual structures, e.g., the acanthite structure of Ag_2S contains both two- and four-coordinate Ag^I, and Au^I exists in two-coordination in AuI and CsAuO. Zn^{II} and Cd^{II} compounds show fairly simple structures although even in ZnO the observed coordination number of 4 differs from that of 6 expected on size criteria. For Hg^{II} compounds unusual structures are again common, for example the cinnabar structure of HgS in which Hg^{II} is two-coordinate. The existence of such complex structures (or their stability with respect to hypothetical simpler structures) has not yet been given an adequate quantum mechanical explanation.

Accurate direct quantum mechanical calculation of the total energies of such complex materials containing heavy atoms is still not possible nor is it likely for some time in the future. Nonetheless, some understanding of these structures can be achieved with use of the qualitative molecular orbital concepts which have been successfully applied to gas-phase molecules.[2] Such an approach relies upon the identification of one or a few orbitals and the investigation of their change in energy as a function of structure type. The basic principle of such a method is to minimize the product of orbital energy times occupation number, e.g., by distorting a symmetric structure in such a way as to stabilize filled orbitals and destabilize empty orbitals. Many such methods in the past have relied upon rather simple quantum mechanical methods such as that of extended Hückel theory.[3] In this work we rely upon orbital energies or ionization potentials obtained either by analysis of X-ray spectral data or from multiple-scattering self-consistent-field Xα (MS–Xα) MO calculations,[4] which have been shown to yield accurate ionization potentials for a wide variety of transition-metal compounds. We feel that this is a critical methodological improvement for the systems under study since the energetic relations between metal (M) d and ligand (L) p orbitals are rather subtle and require rather accurate methods for their prediction. Indeed, for compounds of Au and Hg, consideration of relativistic effects may even be quite important. However, the principles which we finally derive will be qualitative in nature and will therefore not rely upon the detailed features of this computational method.

In the following section the analysis of the spectra and the computations to obtain information on the energies of predominantly M d or L p orbitals in sulfides and chlorides of the Cu and Zn group metals is described, in some cases referring to previous work. When spectral data do not exist, MS–Xα calculations are employed to give approximate in-

(1) Wells, A. F. "Structural Inorganic Chemistry", 4th ed.; Clarendon Press: Oxford, 1975.

(2) Gimarc, B. M. "Molecular Structure and Bonding: The Qualitative Molecular Orbital Approach"; Academic Press: New York, 1979.
(3) Hoffmann, R. *J. Chem. Phys.* **1963**, *39*, 1397.
(4) Johnson, K. H. *Annu. Rev. Phys. Chem.* **1975**, *39*.

0020-1669/81/1320-3333$01.25/0

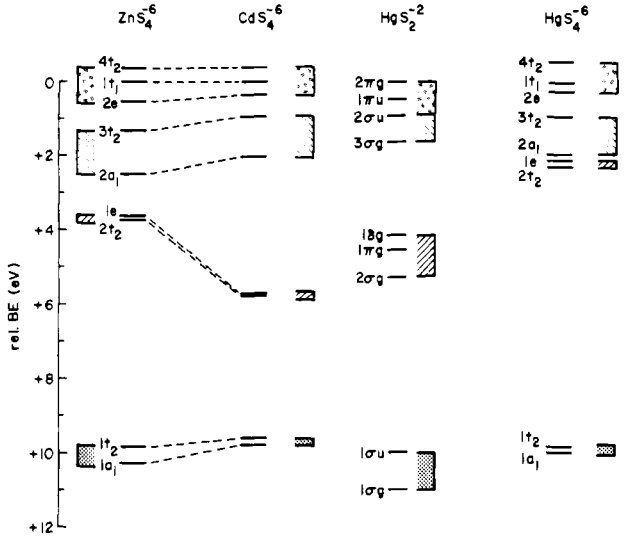

Figure 1. MS–Xα relative ground-state orbital energies (in eV) for ZnS_4^{6-}, CdS_4^{6-}, HgS_2^{2-}, and HgS_4^{6-} (S 3p nonbonding, M–S 3p bonding, M d and S 3s regions specified).

formation on electronic structure. The effects of M coordination number upon M d–L p energy differences are then explored by analyzing spectra or calculations for monomers, polymers, and condensed phases. A discussion is then given of the energetics of M d–L p mixing. Finally, the structures preferred by binary compounds of these metals are explained with use of a simple set of structural principles, which are summarized in the conclusion.

Throughout our discussion we will refer to M d and L p orbitals, but it must be remembered that these labels only specify the largest AO contribution to the molecular orbital. In fact, many of the M d type orbitals have strong ligand p orbital antibonding admixtures and it is precisely this orbital mixing which gives rise to the energetic effects we describe below. In the same way some of the orbitals we describe as L p will have some metal character, usually with M s or M p participation predominant.

Metal d and Ligand p Energies from Calculations and Spectra. Zn, Cd, and Hg Compounds. Calculations have been performed on a series of cluster units with use of the MS–Xα method. Bond distances, sphere radii, and statistical exchange (α) values used are listed in Table V. First the MO energy levels were calculated for the tetrahedral ZnS_4^{6-}, CdS_4^{6-}, and HgS_4^{6-} clusters which can be considered as the basic building blocks of the monosulfide solids which occur in nature as the minerals sphalerite (or also wurtzite), hawleyite (also greenockite), and metacinnabar. A calculation was also performed on the two-coordinated linear HgS_2^{2-} unit which can similarly be considered the basic unit occurring in the mineral cinnabar (HgS). The results of these calculations on sulfides are presented in the energy level diagrams in Figure 1. The MO ground-state energy levels for the cluster units are labeled according to the irreducible representations of the relevant symmetry group. From the calculations, it is also possible to comment on the compositions of particular molecular orbitals in terms of the contribution of atomic orbitals from the metal or sulfur. Thus, for the ZnS_4^{6-} cluster, the $4t_2$, $1t_1$, and 2e orbitals are dominantly S 3p nonbonding orbitals, the $3t_2$ and $2a_1$ orbitals are the main bonding orbitals of the system, and the 1e and $2t_2$ orbitals are the predominantly metal 3d type orbitals. The $1t_2$ and $1a_1$ orbitals are essentially S 3s nonbonding orbitals. The formation of *bands* or collective electron states through overlap between many of these orbitals in a sphalerite crystal is simplistically illustrated in Figure 1 and the character of the bands also shown. In comparing calculations for the different clusters, the $1t_1$ nonbonding S 3p type orbital of the tetrahedral cluster and the S 3p nonbonding $2\pi_g$ orbital of the linear unit have been taken as the zero point on the energy scale.

The validity of calculations of this type can be established by comparison with experimental data derived from spectroscopic measurements. This has already been done in the case of the ZnS_4^{6-} calculation[5] and the calculated energies showed good agreement with experiment. The calculated MO energies for the CdS_4^{6-} cluster also show good agreement with those obtained through the interpretation of published spectra[6,7] of CdS, as illustrated in Table I. Similar comparisons between spectra and calculations are also shown for HgS_2^{2-} in Table I. Valid comparison of calculations with spectra requires the use of the transition-state procedure[8] in which spectral energies

Table I. Orbital Binding Energies Derived from MS–Xα Calculations and from Spectroscopic Measurements for Zinc, Cadmium, and Mercury Sulfides

peak	rel binding energy, eV: measd	calcd	assignt
(a) ZnS_4^{6-} Calculations and ZnS XPS and XES[a]			
I	0	0	$4t_2$, $1t_1$, 2e
II	3.0	1.3, 2.5	$3t_2$, $2a_1$
Zn 3d	7.3	7.6, 7.7	1e, $2t_2$
III	10.3	9.8, 10.2	$1t_2$, $1a_1$
(b) CdS_4^{6-} Calculations and CdS UPS and K_β XES			
I[b]	0[c]	0	$4t_2$, $1t_1$, 2e
II[b]	3.1[c]	1.0, 2.0	$3t_2$, $2a_1$
Cd 4d[b]	8.4[c]	8.3	$2t_2$, 1e
S 3s[b]	10.7[c]	9.8	$1t_2$, $1a_1$
(c) HgS_2^{2-} Calculations and HgS UPS			
I_2, I_4[d]	0, 0.9[d]	0, 0.5, 0.9	$2\pi_g$, $2\sigma_u$, $1\pi_u$
II_2[d]	3.6[d]	1.6	$3\sigma_g$
Hg 5d[d]	6.6[d]	6.6[e]	$2\sigma_g$, $1\pi_g$, $1\delta_g$
		10.2	$1\sigma_u$, $1\sigma_g$

[a] From ref 5. [b] Assignments from ref 6 except for S 3s peak shown to be more tightly bound than Cd 4d in ref 7. [c] I, II, and d from ref 6; S from ref 7; lowest binding peak is reference zero. [d] Reference 6. [e] In nonrelativistic calculation 9.6 eV C corrected for 2.98-eV relativistic change in Hg^0 5d binding energy from ref 9).

Table II. Orbital Binding Energies Derived from MS–Xα Calculations and from Spectroscopic Measurements for Zinc, Cadmium, and Mercury Chlorides

peak	rel binding energy, eV: measd	calcd	assignt
(a) $ZnCl_4^{2-}$ Calculations and $ZnCl_2$ UPS[10]			
Cl 3p (nb)	0	0	$4t_2$, $1t_1$, 2e
Zn–Cl (b)	1.0, 2.6	0.8, 2.4	$3t_2$, $2a_1$
Zn 3d	6.3	7.0	1e, $2t_2$
Cl 3s		11.9, 12.1	$1t_2$, $1a_1$
(b) $CdCl_6^{4-}$ Calculations and $CdCl_2$ XPS and XES[11]			
Cl 3p (nb)	0	0	$3e_g$, $1t_{1g}$, $1t_{2u}$, $3t_{1u}$
Cd–Cl (b)	2.5	0.7, 1.0, 1.9	$2t_{2g}$, $2t_{1u}$, $2a_{1g}$
Cd 4d	7.5	8.9	$1t_{2g}$, $2e_g$
Cl 3s		11.8, 12.0	$1e_g$, $1t_{1u}$, $1a_{1g}$
(c) $HgCl_2$ Calculations and Gaseous $HgCl_2$ UPS[12,13]			
Cl 3p	0, 0.7, 1.3, 2.3	0, 0.3, 0.7	$2\pi_g$, $1\pi_u$, $2\sigma_u$, $3\sigma_g$
Hg 5d	5.3, 7.1	6.3	$1\delta_g$, $1\pi_g$, $2\sigma_g$
Cl 3s		12.4, 13.0	$1\sigma_g$, $1\sigma_u$

(5) Tossell, J. A. *Inorg. Chem.* **1977**, *16*, 2944.
(6) Shevchik, N. J.; Tejeda, J.; Langer, D. W.; Cardona, M. *Phys. Status Solidi B* **1973**, *60*, 345.
(7) Mikhailova, S. S.; Nemnonov, S. A.; Minin, V. I.; Maksyutov, F. B.; Galakhov, V. R. *Izv. Akad. Nauk SSSR, Ser. Fiz.* **1976**, *40*, 439.
(8) Slater, J. C. *Adv. Quantum Chem.* **1972**, *6*, 1.

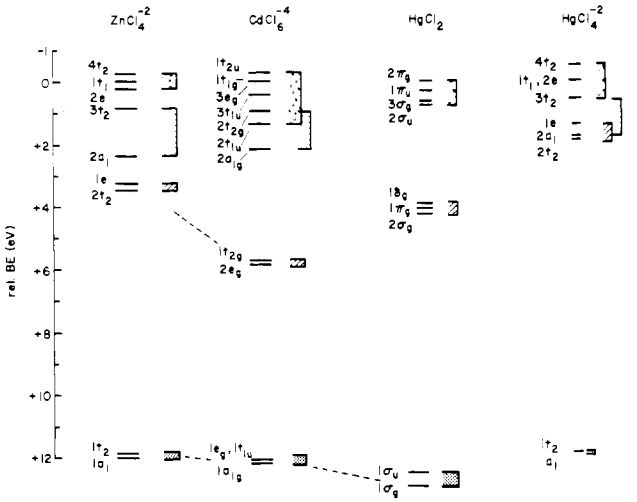

Figure 2. MS-Xα relative ground-state orbital energies for $ZnCl_4^{2-}$, $CdCl_6^{4-}$, $HgCl_2$, and $HgCl_4^{2-}$ (orbital types identified as in Figure 1).

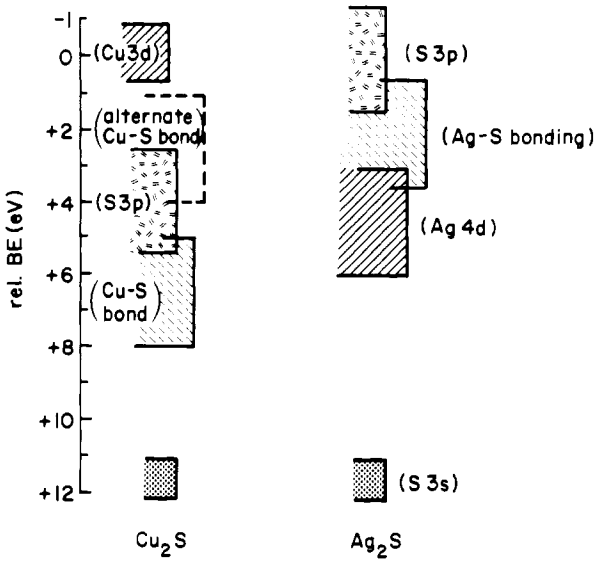

Figure 3. Cu_2S and Ag_2S orbital binding energies from spectra.

are obtained from eigenvalues in "transition states" with occupation numbers intermediate between the initial and final states. All calculated energies in Table I are from transition-state calculations. For HgS the Hg 5d energies have also been crudely corrected for relativistic effects. This has been done by multiplying the difference between the calculated relativistic and nonrelativistic Hg 5d atomic orbital energies[9] (2.98 eV) by the percentage of charge within the Hg atomic sphere in the molecular orbital. For HgS_2^{2-} this gives a destabilization of the $2\sigma_g$ orbital of 2.0 eV while that for the $1\pi_g$ and $1\delta_g$ is 2.8 eV.

For the series of chloride compounds $ZnCl_2$, $CdCl_2$, and $HgCl_2$, similar calculations have been performed with use of the MS-Xα method and results are shown in Figure 2. $ZnCl_2$ contains zinc in tetrahedral coordination to chlorine and occurs in three polymorphs, all of which contain tetrahedral $ZnCl_4$ groups sharing all vertices. In the case of $CdCl_2$, the metal occurs in octahedral coordination to chlorine in a layer structure (the "CdI_2 structure"). The results of a calculation on a $CdCl_6^{4-}$ cluster are shown in Figure 2. The mercury dichloride has a structure in which two chlorines are close to the mercury (2.3 Å) and four more chlorines are more distant neighbors (3.3–3.6 Å). The coordination may be regarded either as twofold or as a very distorted sixfold. For this case calculations have been undertaken on the $HgCl_2$ cluster.

Again the validity of the calculations can be assessed with reference to spectroscopic data such as the UV photoelectron spectrum of $ZnCl_2$,[10] which shows a broad Cl 3p orbital peak at low binding energy and a narrow Zn 3d peak. The Zn 3d and Cl 3p orbitals mix little, partly because of the low Cl 3p binding energy and partly due to the low coordination number of Zn in $ZnCl_2$ (vide infra). In $CdCl_2$ the Md orbitals also generate a narrow corelike peak which is even farther separated from the Cl 3p orbitals than is the case in $ZnCl_2$.

For $HgCl_2$ spectral data is available only for the gaseous triatomic molecule Cl–Hg–Cl, with a Hg–Cl distance of 2.34 Å. The MS-Xα transition-state binding energies are in reasonable agreement with the experimental data after correction has been made for the relativistic lowering of the Hg 5d binding energy.[9] Our results are qualitatively similar to the relativistic ab initio results of Hay et al.,[9] although our analysis is less detailed. Since solid $HgCl_2$ has the highly distorted 2 + 4 coordination described above, we expect the orbital energy separations in solid $HgCl_2$ to be much like those in the gaseous molecule. On the other hand, for the $HgCl_4^{2-}$ cluster, which occurs in several solids, we calculate the separation of Hg 5d and Cl 3p orbitals to be considerably smaller (Figure 2).

Table III. Orbital Binding Energies from MS-Xα Calculations and Spectra for Copper and Silver Sulfides

peak	rel binding energy, eV: measd	rel binding energy, eV: calcd	assignt
	(a) CuS_3^{5-} Calculations[16] and Cu_2S XPS and XES		
A	−3.1, −2.5	−2.9	$4t_2$
B	−1.8, −1.3	−2.0	2e
C	0	0	$1t_1$, $3t_2$, 1e, $2t_2$, $2a_1$
S 3s	8	8.8	$1t_2$, $1a_1$
	(b) AgS_2^{3-} and AgS_4^{7-} Calculations and Ag_2S XPS and XES[14]		
D	0	0–0.5,[a] 0–1.6[b]	S 3p (nb)
C	1.9		Ag–S 3p (b)
B	4.4	7.7,[a] 3.9[b]	Ag 4d
A	11.6	10.1,[a] 10.3[b]	S 3s

[a] AgS_2^{3-}. [b] AgS_4^{7-}.

Cu^I, Ag^I, and Au^I Compounds. Cu_2S exists as the mineral chalcocite in which copper occurs in two kinds of triangular coordination.[14] Sulfur K_β and $L_{2,3}$ X-ray emission spectra, together with X-ray photoelectron spectra, have been published for Cu_2S,[15] and these spectra can be used to construct the empirical energy level diagram shown in Figure 3. In this particular case a calculation is available for comparison with these spectroscopic data; a MS-Xα calculation performed on a triangular CuS_3^{5-} cluster[16] gives transition-state energies which agree well with the experimental data, as shown in Table III. For the CuS_3^{5-} cluster the highest occupied orbitals $4t_2$ and 2e are predominantly Cu 3d in character, the $1t_1$, $3t_2$, and 1e orbitals are essentially S 3p nonbonding in character and the $2t_2$ and $2a_1$ are bonding orbitals of mixed S 3p and Cu 4p or 4s character. Note that the copper and zinc sulfides therefore differ greatly in electronic structure.

Ag_2S as the mineral acanthite has half of the silver atoms in a twofold, nearly linear coordination and half in a distorted

(9) Hay, P. J.; Wadt, W. R.; Kahn, L. R.; Bobrowicz, F. W. *J. Chem. Phys.* **1978**, *69*, 984.
(10) Pong, W.; Okada, S. K. *Phys. Rev. B: Condens. Matter* **1979**, *19*, 5307.
(11) Sugiura, C. *J. Chem. Phys.* **1975**, *62*, 1111.
(12) Eland, J. H. D. *Int. J. Mass Spectrom. Ion Phys.* **1970**, *4*, 37.
(13) Berkowitz, J. *J. Chem. Phys.* **1974**, *61*, 407.
(14) Evans, H. T. *Nature (London), Phys. Sci.* **1971**, *232*, 69.
(15) Domashevskaya, E. P.; Terekhov, V. A.; Marshakova, L. N.; Ugai, Y. A.; Nefedov, V. I.; Sergushin, N. P. *J. Electron Spectrosc.* **1976**, *9*, 261.
(16) Tossell, J. A. *Phys. Chem. Miner.* **1978**, *2*, 225.

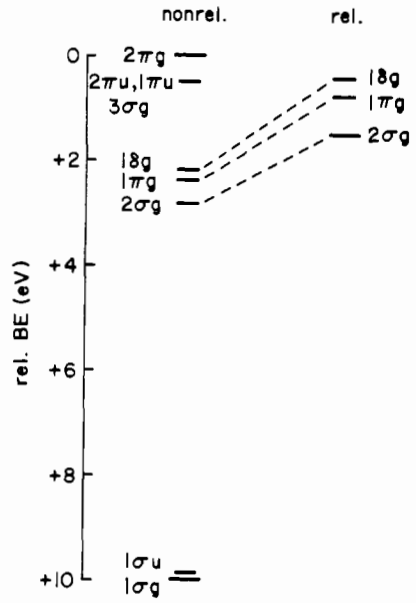

Figure 4. MS–Xα relative ground-state orbital energies for AuS_2^{3-} (in relativistic calculation only the $2\sigma_g$, $1\pi_g$, and $1\delta_g$ orbitals change significantly in energy).

tetrahedral coordination.[17] The energy level diagram for Ag_2S shown in Figure 3 has been constructed from sulfur K_β and $L_{2,3}$ and X-ray photoelectron spectra.[14] MS–Xα orbital energies for the AgS_2^{3-} and AgS_4^{7-} clusters are given in Table III. Although the calculations underestimate the width of the S 3p nonbonding and the Ag–S 3p bonding orbital region, the calculated Ag 4d orbital energy for the AgS_4^{7-} cluster is reasonably close to the experimental value. However, the experimental spectra show no evidence of the tightly bound Ag 4d orbitals predicted for two-coordinate Ag^I. It therefore seems improbable that the Ag_2S studied in the photoemission experiment had the acanthite structure. At high temperature acanthite transforms to argentite, which apparently has Ag^I partly in tetrahedral and partly in octahedral coordination, with no two-coordinate sites. The material studied may be related to this structure.

As has been noted,[15] there is a remarkable inversion of the M d and S 3p levels between Cu_2S and Ag_2S. In the Cu^I compound the Cu 3d orbitals are considerably less tightly bound than are the S 3p nonbonding orbitals while in Ag_2S the Ag 4d orbitals are more tightly bound than the S 3p. No spectral data is available for Au_2S, and its structure is unknown. An MS–Xα orbital energy diagram is presented in Figure 4 for the AuS_2^{3-} cluster. Both nonrelativistic and approximate relativistic ground-state orbital energies are shown (relativistic energies were obtained as in the case of HgS). The orbitals with substantial Au 5d character ($2\sigma_g$, $1\pi_g$, $1\delta_g$) are found to be only slightly more tightly bound than the S 3p nonbonding orbitals. Thus, the Au 5d orbitals are intermediate in energy between Cu 3d and Ag 4d.

Turning to the corresponding chlorides, we find that CuCl has the sphalerite-type structure with copper in tetrahedral coordination and occurs naturally as nantokite. AgCl adopts the halite structure, and hence silver is in ocathedral coordination; the mineral species is cerargyrite ("horn silver"). From X-ray photoelectron spectra for CuCl[18] and related spectra reported in the same publication, the energy level diagram shown in Figure 5 has been constructed. A comparable diagram for AgCl is also shown and the Cu 3d orbital

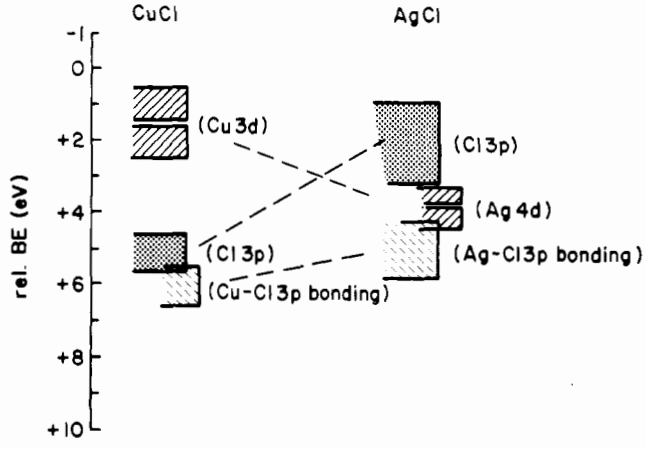

Figure 5. CuCl and AgCl orbital binding energies from spectra.

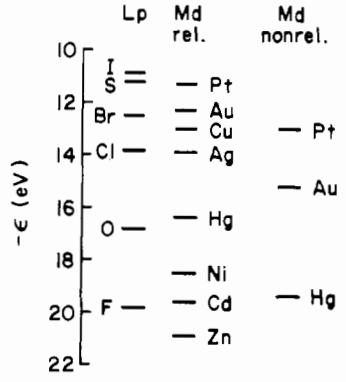

Figure 6. Calculated L p and M d AO energies (from ref 20 and 21).

binding energies are found to be considerably lower than those for the Ag 4d orbitals. Actually, the Ag 4d orbital character is spread over a wide energy range, although the decomposition of the spectral density of states into Ag 4d and Cl 3p contributions (based on the variation of spectral intensity with photon energy) indicates little admixture of Cl 3p character into the main Ag 4d peaks.[19]

Trends in Atomic Orbital Energies. Trends in M 3d orbital energies in the solids discussed above can be understood to some extent in terms of their orbital energies in the isolated atoms. In figure 6 atomic orbital (AO) energies from relativistic Hartree–Fock calculations[20] are given for M d and L p orbitals. For Pt, Au, and Hg we also give nonrelativistic Hartree–Fock orbital energies.[21] The lower binding energy of S 3p vs. Cl 3p nonbonding orbitals is understandable from these atomic results which show a S 3p–Cl 3p binding energy difference comparable to that observed in solids. The low stability predicted for the Au 5d orbitals in solids and that observed for the Hg 5d are also explicable in terms of the low binding energies of the free atom orbitals. This effect is primarily a relativistic one and has been carefully discussed.[9,22,23] However the greater stability of Cd 4d vs. Zn 3d levels in solids is opposite in direction to the orbital energy difference in the free atoms, and the Ag 4d vs. Cu 3d free atom orbital energy difference is considerably smaller than the difference observed in solids, although the trend is in the same direction. MS–Xα transition-state calculations indicate that

(17) Frueh, Jr., A. J. *Z. Kristallogr.* **1958**, *110*, 136.
(18) Kono, S.; Ishii, T.; Sagawa, T.; Kobayasi, T. *Phys. Rev. B: Solid State* **1973**, *8*, 795.
(19) Tejeda, J.; Braun, W.; Goldman, A.; Cardona, M. *J. Electron Spectrosc.* **1974**, *5*, 583.
(20) Desclaux, J. P. *At. Data Nucl. Data Tables* **1973**, *12*, 311.
(21) Mann, J. B. "Atomic Structure Calculations I", Hartree-Fock Energy Results for the Elements Hydrogen to Lawrencium; USAEC Los Alamos Scientific Laboratory, Los Alamos, NM, 1967; LA-3690.
(22) Pitzer, K. S. *Acc. Chem. Res.* **1979**, *12*, 271.
(23) Pyykko, P.; Desclaux, J. *Acc. Chem. Res.* **1979**, *12*, 276.

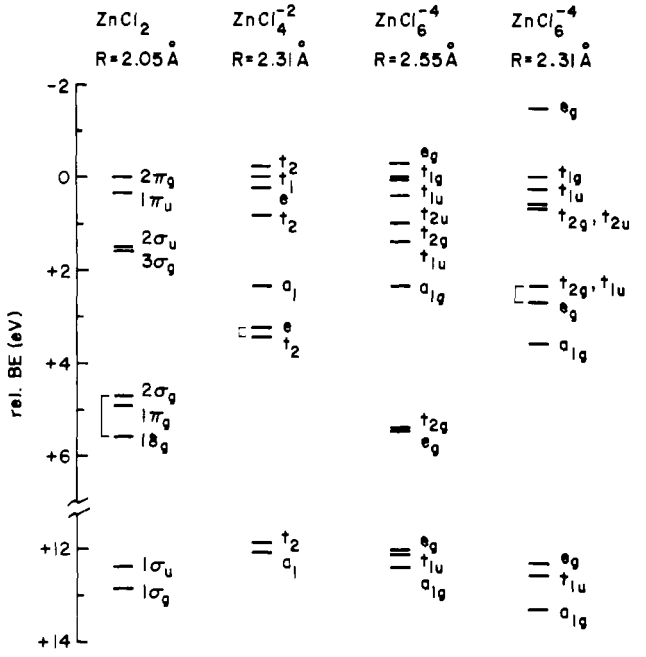

Figure 7. MS–Xα relative ground-state orbital energies for $ZnCl_2$, $ZnCl_4^{2-}$, and $ZnCl_6^{4-}$ (R = 2.55 and 2.31 Å).

a large part of the difference between Cu 3d and Ag 4d binding energies arises not from ground-state energy differences but from the considerably larger relaxation calculated for the Ag 4d orbitals in the photoionization transition state.

Relative Energies of M d and L p Orbitals as a Function of Coordination Number. We have previously observed[5] that the separation of Zn 3d and F 2p orbitals is much larger in the linear triatomic molecule ZnF_2 than in solid ZnF_2, in which Zn is six-coordinate, and we have attributed most of this difference to the difference in Zn coordination number. A similar effect occurs for $ZnCl_2$. In Figure 7 we present MS–Xα calculated orbital energies for $ZnCl_2$ and $ZnCl_4^{2-}$ and for $ZnCl_6^{4-}$ at two different Zn–Cl distances. Clearly the transition from two- to four-coordination causes a substantial raising of the Zn 3d type orbitals. In $ZnCl_2$ the calculated binding energy difference between the highest occupied orbital ($2\pi_g$) and the Zn 3d orbitals is 8.2–8.9 eV with the σ-type Zn 3d orbital at lowest binding energy. The energy difference obtained from UPS[24] for gaseous $ZnCl_2$ is 7.3–7.5 eV, which is indeed larger than the 6.3-eV Cl 3p–Zn 3d energy difference observed for solid $ZnCl_2$[10] with four-coordinate Zn. However, further increase of coordination number to 6 has no clear effect upon the Zn 3d–Cl 3p orbital energy separation. This separation can be either larger or smaller than that in the four-coordinate form depending upon the Zn–Cl distance chosen. For a Zn–Cl distance 0.12 Å greater in the six-coordinate form the Zn 3d–Cl 3p energy difference is quite similar to that in four-coordination. It was previously noted[5] that the Zn 3d–S 3p energy separation did not differ much for calculations on ZnS_4^{6-} and ZnS_6^{10-}. This suggests that the most important destabilization of the Zn 3d levels occurs in the change from one- to two-coordination in the gaseous molecule to four-coordination in the solid.

A similar difference is observed between the energy level orderings in the linear triatomic molecules MnF_2 through NiF_2[25] compared to those in solids with the same stoichiometry,[26] in which the transition-metal atoms are six-coordinate. Spin-polarized calculations on $MnCl_2$ indicate that the σ component of the Mn 3d orbital is more stable than the Cl 3p nonbonding levels and that the average binding energy of the predominantly Mn 3d levels is slightly higher than that of the highest Cl 3p nonbonding level. For solid $MnCl_2$, the t_{2g} symmetry Mn 3d orbital lies more than 1 eV above the Cl 3p nonbonding orbitals, and the separation in average energy between Cl 3p and Mn 3d is more than 2 eV. Similarly for gaseous $NiCl_2$, the calculations indicate that the δ symmetry Ni 3d orbitals and the nonbonding Cl 3p orbitals will be at about the same energy, while the spectrum of the solid indicates all the Ni 3d levels to be less tightly bound than the Cl 3p. The closeness in energy of the M 3d and Cl 3p orbitals in the triatomic molecules makes electronic structure calculations difficult since a number of different orbital configurations are close in energy.

Dramatic changes also occur in the relative M d and L p orbital energies for molecules such as CuCl and AgCl in passing from diatomic molecule to gas-phase trimer to solid. In gaseous AgCl, the Ag 4d orbitals have binding energies around 14 eV and are well separated from the Cl 3p orbitals with binding energies of 10–11 eV.[27] Cellular-Xα calculations on the AgCl diatomic using the transition-state procedure satisfactorily reproduced the spectral results.[27] Different experimental conditions favor the formation of $(AgCl)_3$ and yield spectra showing two additional peaks intermediate in binding energy between the Cl 3p and Ag 4d features in the diatomic.[28] On the basis of intensity variations between He I and He II excitation, it was determined that the new peak at 12.6 eV was mainly of Ag 4d character. The spectrum therefore reflects a somewhat reduced Cl 3p–Ag 4d separation, although the estimated mixing of Cl 3p and Ag 4d character remains small in all the orbitals. For the case of solid AgCl a similar analysis gives a Ag 4d contribution to the density of states which is intermediate in energy between two parts of the Cl 3p density of states.[19] Thus, the Ag 4d orbitals are much higher in energy with respect to the Cl 3p in the solid and are much more strongly mixed with them. This means that the Ag 4d orbitals are considerably more stable than the Cl 3p in the diatomic molecule and rise in relative energy when the Ag coordination number increases.

For CuCl a similar change occurs. Cellular-Xα calculations on the diatomic molecule[27] show the Cu 3d orbitals to be slightly less tightly bound than the Cl 3p and well mixed with them. Condensation to the trimer and then to the solid should raise the Cu 3d orbital energies and reduce the amount of mixing. Potts and Lyus[28] indeed observed distinct Cu 3d and Cl 3p orbital sets for $(CuCl)_3$ and CuCl(s) with the Cu 3d features occurring at lower binding energy. They also found a somewhat larger Cu 3d–Cl 3p average separation in the solid, and their overall results for the series CuCl, CuBr, and CuI indicate less Cu 3d–L p mixing in the solid than in the trimer. Since the Cu 3d orbitals are less tightly bound than the Cl 3p in the diatomic molecule, it is expected that condensation will increase this energy separation and reduce the amount of orbital mixing.

Another strong effect on the M 3d–L p separation of course arises from changes in the identity of the ligand. X-ray emission spectra of solids[29] lead to average L p nonbonding orbital energies of about 7, 8, 4, and 7 eV for O, F, S, and Cl, respectively. Thus, the M d–L p separation will be smallest in the sulfide if the M d orbitals are less strongly bound that the L p (e.g., Cu) and smallest in the fluoride if the M d levels lie deeper than the L p (e.g., Ag, Zn, Cd, Hg). This effect is most easily seen in the very small separation of M d and

(24) Orchard, A. F.; Richardson, N. V. *J. Electron Spectrosc.* **1975**, *6*, 61.
(25) Berkowitz, J.; Streets, D. G.; Garritz, A. *J. Chem. Phys.* **1979**, *70*, 1305.
(26) Poole, R. T.; Riley, J. D.; Jenkin, J. G.; Liesegang, J.; Leckey, R. C. G. *Phys. Rev. B: Solid State* **1976**, *13*, 2620.
(27) Berkowitz, J.; Batson, C. H.; Goodman, G. L. *J. Chem. Phys.* **1980**, *72*, 5829.
(28) Potts, A. W.; Lyus, M. L. *J. Electron Spectrosc.* **1978**, *13*, 305.
(29) Koster, A. S.; Mendel, H. *J. Phys. Chem. Solids* **1970**, *31*, 2523.

L p levels in Cu_2S and AgCl. It has also been noted previously that significant Zn 3d, F 2p orbital mixing occurs in ZnF_2.

Recently both UPS[10] and FK_α XES[30] studies have been performed on ZnF_2 and can be used in conjunction with previous calculations[5] and XPS studies[31] to understand the nature of Zn 3d–F 2p mixing. The FK_α XES, combined with a determination of the F 1s binding energy and the valence region XPS, shows the main FK_α peak, associated with the F 2p nonbonding orbitals, to lie about halfway between the two peaks seen in the XPS spectrum. This supports the interpretation of the two XPS peaks as arising from the Zn 3d–F 2p bonding and antibonding orbital sets. The larger intensity of the lower binding energy peak in UPS as contrasted to XPS is explained by the greater amount of F 2p character in the antibonding orbitals compared to that in the bonding orbitals (76% compared to 11%).

Energetic Effect of M d, L p Interaction. The mixing of metal d and ligand p orbitals generates bonding and antibonding molecular orbitals. The application of second-order perturbation theory to those cases in which the interaction is small shows the splitting of bonding and antibonding levels to be proportional to the square of the orbital overlap and inversely proportional to the difference of atomic orbital energies. Such relations are also expected to be qualitatively valid for larger interactions. It is generally observed that, if both the bonding and antibonding orbitals arising from the interaction of atomic orbitals are completely filled, the overall interaction is destabilizing. On the other hand, if the most strongly antibonding MO's are empty, a net stabilization may result. Thus we would expect systems having completely filled M d–L p antibonding orbitals to adopt structures in which M d–L p interaction was minimized and those with partially empty antibonding sets to adopt structures maximizing this interaction.

The magnitude of the interaction is dependent first upon the nature of the ligand since this will strongly influence both the orbital overlap and the AO energy difference. However, it is also dependent upon coordination number and detailed geometry. A higher coordination number will tend to raise the M d orbital energies compared to the L p. This may either increase or decrease the M d–L p energy difference, depending upon whether the M d orbitals lie above or below the L p. Thus, systems with filled antibonding orbitals will tend to prefer high coordination numbers if the M d levels tend to lie above the L p and low coordination numbers if they lie below. This effect will be greatest when the L p levels overlap strongly with the M d and do not differ greatly from them in energy.

Systems with partially empty antibonding levels will tend to prefer structures in which the M d and L p orbitals interact strongly. For a given coordination number they will also prefer the ligand arrangement which gives the maximum separation of the M d–L p antibonding orbitals with different symmetries; e.g., they will prefer square-planar rather than tetrahedral geometries.

Analysis of Structural Preferences. The most stable polymorphs of many binary compounds of Ni, Pd, Pt, Cu, Ag, Cu, Zn, Cd, and Hg are briefly described in Table IV. For the fluorides an increase in coordination number of the metal down the Zn^{II}, Cd^{II}, Hg^{II} series is observed, as expected from the ionic model for an increase in cation to anion radium ratio. This suggests that the mixing of F 2p with the M d orbitals is not strongly destabilizing, no matter what the metal atom. It is also observed that of the Cu^{I}, Ag^{I}, Au^{I} series only Ag^{I} forms a fluoride stable enough to be characterized. On the other hand, Cu^{II} and Ag^{II} form stable fluorides, while AuF_2 is unknown. Similarly, PtF_2 is unknown although Pt^{IV} commonly occurs in six-coordination and NiF_2 and PdF_2 adopt the rutile structure. These observations can be explained to a large extent by analysis of the relative energies of the relevant AO's.

For a structure to be stable all partially occupied orbitals are expected to have more positive binding energies than the completely occupied orbitals. We might also expect that the compounds most favored by ionic interactions will be those with the highest charges. Thus, on purely ionic grounds CuF_2 would be more stable than CuF. From this point of view a more surprising aspect of the stability relations in the copper halides is the nonexistence of CuI_2. Study of the copper(I) halides by XPS[18] shows that the I 5p levels are quite close to the Cu 3d levels while in CuCl the Cl 3p to Cu 3d separation is 3–4 eV. Since the Cu 3d levels are stabilized by about 2 eV in going from Cu^{I} to Cu^{II}, it appears that the partially occupied Cu 3d orbital in Cu^{II} must drop below the I 5p, creating an unstable electron configuration. In fact, if the Cu^{II} coordination were regular octahedral, such instability would result even for the lighter halogens. A distorted 4 + 2 geometry (four short bonds, two long) gives a larger symmetry splitting within the Cu 3d–L p antibonding orbital manifold so that the half-occupied highest energy Cu 3d–L p orbital lies above the L p nonbonding orbital.

Table IV. Observed Metal Coordination Numbers for Cu and Zn Family Compounds

	F	Cl	Br	I	O	S
Cu^{I}	...	4 T	4 T	4 T	2	3
Ag^{I}	6	6	6	4 T	2	2, 3
Au^{I}	?	?	?	2	2	4?
Cu^{II}	4 + 2 (ΔR = 0.34)	4 + 2 (ΔR = 0.65)	4 + 2 (ΔR = 0.78)	...	4 SP	3, 4
Au^{III}	4 SP	4 SP	4 SP	?	?	?
Zn^{II}	6	4 T	4 T	4 T	4 T	4 T
Cd^{II}	8	6	6	6	6	4 T
Hg^{II}	8	2 + 4 (ΔR = 1.2)	2 + 4 (ΔR = 0.7)	2 + 4, 4 (ΔR = 0.9)	2	2
Ni^{II}	6	6	6	?	6	6
Pd^{II}	6	4 SP	4 SP	?	4 SP	4 SP
Pt^{II}	...	4 SP	...	...	...	4 SP

[a] ... signifies compound is unknown, ? signifies compound exists but structure is unknown, T = tetrahedral, SP = square planar, 4 + 2 = four short and two long bonds, and 2 + 4 = 2 short and 4 long bonds (ΔR in A, data from ref 1).

Table V. M-L Distances, R, and Sphere Radii, RS (in A), Employed in MS-Xα Calculations[a]

		RS	
	R(M-L)	M	L
CuS_3^{5-}	2.19	1.37	1.44
AgS_2^{3-}	2.51	1.44	1.31
AgS_4^{7-}	2.84	1.64	1.51
AuS_2^{3-}	2.65	1.75	1.51
ZnS_4^{6-}	2.34	1.39	1.48
$ZnCl_2$	2.05	1.23	1.32
$ZnCl_4^{2-}$	2.31	1.36	1.48
$ZnCl_6^{4-}$	2.31	1.36	1.48
$ZnCl_6^{4-}$	2.55	1.22	1.33
CdS_4^{6-}	2.52	1.53	1.48
$CdCl_6^{4-}$	2.74	1.53	1.75
HgS_2^{2-}	2.36	1.48	1.32
HgS_4^{6-}	2.53	1.59	1.42
$HgCl_2$	2.25	1.32	1.16
$HgCl_4^{2-}$	2.50	1.59	1.51

[a] All α values taken from ref 35; outer-sphere radius tangent to ligand sphere.

(30) Esmail, E. I. "A Study of the Bonding in Fluorine Compounds Using X-ray Emission and Photoelectron Spectroscopies", unpublished Ph.D. Thesis, Queen Mary College, University of London, England, 1975.
(31) Nyholm, R. S. *Proc. Chem. Soc. London* **1961**, *273*.

For Ag^{II}, the d orbitals of which are more tightly bound than those of Cu^{II}, only in AgF_2 can the partially occupied Ag 3d orbital lie above the L p nonbonding orbital. Therefore, even though AgCl, AgBr, and AgI are not particularly stable due to the destabilizing influence of the filled d shell, they are competitive in energy with the hypothetical dihalides. For Au^{I} the only halide stable enough to be characterized is AuI, which has the least tightly bound L p orbitals within the halides giving a larger Au 5d–L p separation and consequently a smaller destabilization of the closed Au 5d shell. The nonexistence of Au^{II} compounds suggests that the partially occupied Au 5d type orbital in such hypothetical compounds will be more stable than some occupied ligand orbitals. For Au^{III} compounds this orbital is empty and is strongly destabilized due to short Au–L distances. The strong mixing of Au 5d and L p orbitals and the low binding energy of the Au 5d AO ensure that this unoccupied orbital will lie above the L p for AuF_3, $AuCl_3$, and $AuBr_3$. AuI_3 is apparently unknown, suggesting that all of the predominantly Au 5d levels, including the empty one, would lie below the I 5p.

Similar relations are observed for divalent and tetravalent Ni, Pd, and Pt. Due to the high binding energy of its 3d AO, Ni can achieve the +4 oxidation state only in coordination with F, as in K_2NiF_6. Pt, on the other hand, forms tetravalent compounds even with I, and the stability of PtF_4 and PtO_2 are such that PtF_2 and PtO have not been obtained in pure form. Pd is similar to Ni in the oxidation states it adopts. However, since the ligand field splittings of its d orbitals are larger than those in Ni^{2+}, it often has a spin-paired d^8 configuration, as in PdS, and adopts distorted geometries which stabilize the filled while destabilizing the single empty Pd 4d orbital.

Preferred coordination numbers in these compounds can also be understood with use of this qualitative description of M d–L p interactions. For Zn^{II} the destabilizing effect of Zn 3d–L p interaction of the filled electronic shell seems small, but it may be partly responsible for the preference of four coordination in $ZnCl_2$, ZnO, and ZnS. As noted previously, the M d–L p energy separation does not vary greatly between four and six coordination, and its exact value is dependent on M–L distance. For Cd^{II} the destabilization of the filled shell is even smaller as indicated by the large Cd 4d–L p separations observed in the spectra of CdS and $CdCl_2$, consistent with the preference of Cd for high coordination numbers in its chloride and oxide. In Hg, relativistic effects cause the 5d levels to be less tightly bound thus reducing their energy separation from and increasing their mixing with the L p, giving greater destabilization. This destabilization may be reduced by lowering the Hg coordination number. This is certainly one effect contributing to the low coordination numbers observed in most Hg compounds. For Cu^{I} compounds, the same arguments suggest that the high coordination numbers should be favored. In the halides Cu is four-coordinate, in the sulfide it is three-coordinate, but in Cu_2O it is two-coordinate. Since the O 2p binding energy is fairly high, even a small Cu coordination number gives an adequate separation of O 2p and Cu 3d type orbitals, as is seen in the UPS of Cu_2O.[32]

For Ag^{I}, whose d orbitals are more tightly bound than those of Cu^{I}, the degree of destabilizing M d–L p mixing may be limited by either high or low coordination number depending upon the ligand. For ligands which have low binding energy p orbitals, e.g., S and I, low coordination number structures cause the Ag 4d orbitals to be more stable than the ligand p. We have already noted this orbital ordering in Ag_2S, and it has also been observed in AgI.[19] For more electronegative ligands such as F and Cl, structures with Ag^{I} in six-coordination are preferred. As noted previously for solid AgCl, this produces an orbital structure in which the Ag 4d orbitals are slightly less tightly bound than the Cl 3p. The orbital structure for the hypothetical four-coordinate form of AgCl should be intermediate between the observed for $(AgCl)_3$ and six-coordinate AgCl, placing the Ag 4d and Cl 3p levels at about the same energy and thus maximizing the mixing between them.

The variation in bond length distortion in the copper(II) halides also has a simple qualitative explanation in terms of our model. Since the Cu 3d levels are less tightly bound than the L p, the M 3d–L p separation will decrease as the ligand p orbital binding energy decreases along the series from F to Br. In order for the one partially empty Cu 3d orbital to have a lower binding energy than any of the L p orbitals, this orbital will have to be destabilized with respect to the Cu 3d orbital energy baricenter by increased distortion away from octahedral symmetry.

Previous Explanations of Structures Based on Hybridization Arguments. Alternative qualitative explanations for the low coordination numbers often observed in Cu^{I}, Ag^{I}, Au^{I}, and Hg^{II} compounds have been given.[31] It was first asserted that Au and Hg have exceptionally large valence s–p separations due to relativistic stabilization of the 6s shell. This suggests hybridization with increased s character, e.g., sp rather than sp^3, leading to a preference for linear geometries.[31] This interpretation has been challenged by Orgel[32] who noted that the Hg 6s–6p separation was really little different from the Zn 4s–4p separation. However, since the $(n-1)$d–ns separations of Zn and Hg were greatly different, Orgel felt that the d–s hydridization in Hg compounds would provide a better explanation for their low coordination numbers. Although 6s orbital involvement is certainly increased by relativistic effects in Au and Hg compounds, our calculations and the spectral data do not indicate that this effect should favor low coordination numbers. For example, in $HgCl_2$ the only orbital with substantial Hg 6s character is the $3\sigma_g$ which UPS shows to be more tightly bound than $2\pi_g$ by only about 2.3 eV, identical with the $2\pi_g$–$3\sigma_g$ separation observed in $ZnCl_2$. In addition, our nonrelativistic MS–Xα studies on $HgCl_2$ and $HgCl_4^{-2}$ show that the Hg s–Cl p bonding orbital in $HgCl_4^{2-}$ ($2a_1$) has almost as much Hg 6s character as does the $3\sigma_g$ in $HgCl_2$ and is actually more stable with respect to the Cl 3p nonbonding orbital. Incorporation of relativistic effects stabilizing the Hg 6s orbitals should therefore confer at least as much additional stability on the four-coordinate species as on the two-coordinate. A comparison of calculated MS–Xα orbital energies for the tetrahedrally coordinated sulfides of Zn^{II} (Figure 1), Cu^{I}, (16) and Ag^{I} (Table III) shows that the stability of the a_1 bonding orbital, with some M s character, is actually greater for Zn^{II} than for Cu^{I} or Ag^{I}, suggesting less M s involvement for the metals which typically show small coordination numbers. Therefore, although differences in s orbital involvement may play some role in determining coordination numbers our results suggest that differences in d orbital energies and overlaps will be the dominant effect.

Implications. Our calculations indicate that M d–L p orbital energy differences may be modified by changing the M–L distance (viz. Figure 7). The application of pressure may therefore change the stabilities of the compounds discussed. CuI_2 would be a stable compound if the Cu–I distance were reduced enough to drive the partially empty Cu 3d type orbital above the I 5p orbitals. Thus, CuI_2 may become a stable phase at high pressure. Similarly, high pressure may destabilize the Cu 3d orbitals sufficiently to make CuF_3 stable and destabilize

(32) Orgel, L. E. *J. Chem. Soc.* **1958**, 4186.
(33) Kowalczyk, S. P.; Ley, L.; McFeely, F. R.; Pollak, R. A.; Shirley, D. A. *Phys. Rev. B: Solid State* **1974**, *9*, 381.
(34) Benndorf, C.; Caus, H.; Egert, B.; Seidel, H.; Thieme, F. *J. Electron Spectrosc.* **1980**, *19*, 77.
(35) (a) Schwarz, K. *Phys. Rev. B: Solid State* **1972**, *5*, 2466. (b) Schwarz, K. *Theoret. Chim. Acta* **1974**, *34*, 225.

the Au 5d orbitals enough to produce AuI_3. $AgCl_2$, $AgBr_2$, and AgI_2 will also be favored by high pressure. For Hg^{II} compounds a reduction in Hg-L distance will lead to a reduced Hg 5d-L p separation and a stronger destabilization. Such destabilization could be reduced by disproportionation to Hg^{I} and Hg^{III}, both of which might have larger Hg 5d-L p separations than the original Hg^{II} compound. The above effects would occur whether the application of pressure lead to only a gradual reduction in M-L or to a transformation to a higher coordination number polymorph, since distance reduction and coordination number increase have similar effects upon M d orbital energies (so long as the initial coordination number is small).

Conclusion. Analysis of quantum mechanical calculations and X-ray spectra of binary compounds of Cu and Zn family metals indicates individual members differ significantly in M d-L p energy separation and the extent of M d-L p orbital mixing. For the heaviest members of the families, Au and Hg, the M d levels are raised significantly by relativistic effects. In addition to its dependence on metal and ligand identity, the M d-L p energy separation is strongly influenced by M coordination number resulting in significant differences in M d-L p separation between gaseous molecules and solids of the same stochiometry. It appears that many aspects of the structures of Cu and Zn family compounds can be understood on the basis of the following simple principles: (1) Ionic forces favor higher oxidation states. (2) An oxidation state is stable only if all unoccupied M d orbitals (if any) lie above the L p nonbonding orbitals in energy. (3) The average energies of M d orbitals are lowered 1-2 eV by a unit increase in oxidation state. (4) An oxidation state increase therefore decreases the M d-L p energy difference for Cu, increases it for Ag, Au, and Hg, and gives little percentage increase in its initially large value for Zln and Cd compounds. (5) Compounds with one empty or partially filled M d orbital will distort so as to destabilize this orbital, with the effect increasing as the M d-L p separation decreases. (6) Compounds with completely filled M d shells and small M d-L p energy differences will adopt structures whose coordination numbers yield maximum M d-L p energy differences and minimum M d-L p orbital mixing. For Cu compounds this effect will tend to favor large coordination numbers while for Au, Ag, and Hg low coordination numbers will be favored.

Acknowledgment. This work was supported by NASA, Grant No. NSG-7482, and NATO, Grant No. 1509. Computer costs were partly supported by the Computer Science Center, University of Maryland.

Registry No. ZnS_4^{6-}, 63915-41-3; CdS_4^{6-}, 78279-97-7; HgS_2^{2-}, 26015-93-0; HgS_4^{6-}, 78279-98-8; $ZnCl_4^{2-}$, 15201-05-5; $CdCl_6^{4-}$, 44433-10-5; $HgCl_2$, 7487-94-7; $HgCl_4^{2-}$, 14024-34-1; Cu_2S, 22205-45-4; Ag_2S, 21548-73-2; AgS_2^{3-}, 78279-99-9; AgS_4^{7-}, 78280-00-9; AuS_2^{3-}, 78280-01-0; CuCl, 7758-89-6; AgCl, 7783-90-6; $ZnCl_2$, 7646-85-7; $ZnCl_6^{4-}$, 63344-34-3.

Contribution from Bell Laboratories,
Murray Hill, New Jersey 07974

Excitation, Ionization, and Fragmentation in Dimethylmercury

A. GEDANKEN, M. B. ROBIN,* and N. A. KUEBLER

Received January 13, 1981

Unlike the situation in metal carbonyls where M^+ ions result from multiphoton ionization (MPI) of the photoproduced metal atoms, the MPI of $Hg(CH_3)_2$ proceeds through the parent molecular ion $Hg(CH_3)_2^+$ which then photofragments to yield Hg^+. This is demonstrated by the absence of Hg(I) atomic lines in the MPI spectrum and also by mass spectrometry wherein a considerable quantity of molecular parent ion is observed at low laser flux while at high flux this is replaced totally by Hg^+. The MPI spectrum of $Hg(CH_3)_2$ in a jet-cooled, seeded molecular beam displays a two-photon-allowed/one-photon-forbidden Rydberg excitation ($A_1' \rightarrow E''$) in the 51 000-56 000 cm^{-1} region. The Jahn-Teller splitting (14 cm^{-1}) of the $\nu_{11}(1,1)$ sequence bands in the upper state of this transition confirms its E'' spin-orbit assignment. Clustering in the beam removes the sharp-line MPI features totally, as appropriate for a Rydberg excitation. The inelastic electron-impact spectrum of $Hg(CH_3)_2$ also was recorded up to 30-eV loss, and the transitions were assigned with due regard for the strong spin-orbit splitting within the one-electron configurations and the Rydberg term-value concept.

Pulsed-laser irradiation of several transition-metal carbonyls recently has uncovered some rather unexpected results.[1-3] In particular, though the one-photon electronic spectra of the transition-metal carbonyls are generally so broad that no vibrational structure is discernible, the same compounds when studied by the multiphoton ionization (MPI) spectroscopic technique[4] yield a tremendous number of very sharp lines. As shown by Vaida et al.[2,5] these lines are due to MPI processes in the bare metal atom, and, indeed, the MPI mass spectra are strongly dominated by the presence of M^+ ions formed by photoionization.[1,3] On the other hand, $M(CO)_6^+$, $M(CO)_5^+$, ..., etc. are abundant in the electron-impact mass spectra of the same materials.[6] By way of explanation, it appears that the first two photons are absorbed coherently in the transition-metal carbonyls, followed by a rapid loss of CO ($>10^{12}$ s^{-1}) in this and in subsequent incoherent absorption steps. Even though enough energy is pumped into the molecular system to ionize it, the competing dissociation to M + 6CO is overwhelmingly the favored path kinetically, and only M^+ ions form on further absorption of light. Using 3546-Å laser pulses (3546 Å = 3.496 eV) and a time-of-flight mass spectrometer, we have observed only monoatomic M^+ ions when irradiating $Cr(CO)_6$ (17.07 eV), $Mo(CO)_6$ (19.63), $W(CO)_6$ (22.25), $V(CO)_6$ (15.5), $Fe_2(CO)_9$, $Mn_2(CO)_{10}$ (22.13), and $Co_2(CO)_8$ (16.9). The M^+ appearance potentials[7] are given in parentheses. Most recently, this metal-ion-only effect has been

(1) M. A. Duncan, T. G. Dietz, and R. E. Smalley, *Chem. Phys.*, **44**, 415 (1979).
(2) D. P. Gerrity, L. J. Rothberg, and V. Vaida, *Chem. Phys. Lett.*, **74**, 1 (1980).
(3) G. J. Fisanick, T. S. Eichelberger, IV, N. A. Kuebler, and M. B. Robin, submitted for publication in *J. Chem. Phys.*
(4) P. M. Johnson, *Acc. Chem. Res.*, **13**, 20 (1980).
(5) L. J. Rothberg, D. P. Gerrity, and V. Vaida, submitted for publication in *J. Chem. Phys.*
(6) G. A. Junk and H. J. Svec, *Z. Naturforsch. B: Anorg. Chem., Org. Chem., Biochem., Biophys., Biol.*, **23B**, 1 (1968).
(7) H. M. Rosenstock, K. Draxl, B. W. Steiner, and J. T. Herron, *J. Phys. Chem. Ref. Data, Suppl.*, **6** (1977).

0020-1669/81/1320-3340$01.25/0